Transmuting the blue fluorescence of hekates mesogens derived from Tris(N-salicylideneaniline)s core via ZnS/ZnS:Mn^{2+} semiconductor quantum dots dispersion

D. P. Singh,[*][a] A. K. Misra,[b] A. S. Achalkumar,[c] C. V. Yelamaggad,[d] and M. Depriester[a]

[a] Unité de Dynamique et Structure des Matériaux Moléculaires (UDSMM), Université du Littoral Côte d'Opale, 59140 Dunkerque, France.

[b] Physics Department, Govt. V.Y.T. P.G. Autonomous College, Durg 491001, Chhattisgarh, India.

[c] Department of Chemistry , Indian Institute of Technology Guwahati, Guwahati-781039, Assam, India.

[d] Centre for Nano and Soft Matter Sciences, Jalahalli, Bangalore, 560 013, India.

Abstract

In this paper, we present the preparation of nano-soft composites of ZnS and ZnS:Mn^{2+} quantum dots (QDs) with star shaped hekates mesogens (HMs) derived from tris(N-salicylideneaniline) core. The photophysical studies of the neat HMs and it's composites with QDs have been carried out as a function of temperature. The blue emission of HMs is found to be enhanced and red shifted in the presence of ZnS QDs. An induced yellow emission at 575 nm has been observed in HM$-$ZnS:Mn^{2+} QDs composite which is attributed to the ^{4}T$_1$ to ^{6}A$_1$ transition between the sp electrons of ZnS and d electrons of Mn^{2+} in the ZnS:Mn^{2+} QDs. The change in photophysical properties of HMs is analogous to the adscititious electron-proton interactions in hydrogen bonded environment after the dispersion of QDs. The large shift in N$-$H stretching and induction of a new S$-$H stretching band at 2734 cm^{-1} in the composites reveal the occurrence of intermolecular interactions between the HMs and QDs. Moreover, the presence of QDs significantly changes the molecular orientation of the HMs

*Corresponding author, Tel.:+33321465781, Email: Dharmendra.singh@univ-littoral.fr, dpsr4u@gmail.com (D. P. Singh)

as adduced by polarized optical microscopy. Tunability of the blue emission of HMs due to QDs dispersion depends on the degree of intermolecular interactions in the Guest-Host system. This study depicts its possible applications in the quantum dots based tunable photoluminescent displays.

Keywords: `Quantum dots`, Star-shaped mesogens, photoluminescence

---

1. Introduction

After the discovery of Discotic liquid crystal (DLC) by S. Chandrashekhar et al. in 1977, this class of LCs became an adoptive option for zone refined single crystals [1, 2, 3]. DLCs have shown their potential utilization in the self healing process to control the molecular ordering and defects [4]. In last few years, these materials have been eventuated in photo-luminescent and opto-electronic devices [5, 6, 7]. Until now, a large number of DLCs have been designed and characterized to realize the columnar LCs capable of exhibiting high charge carrier mobilities [8, 9, 10, 11, 12]. Non-discotic mesogens, having similar geometrical structures to that of discotics, have attracted particular interest due to their rich photoluminescence properties. Yelamaggad et al. [13] have reported the supramolecular tris(N-salicylideneaniline)s (TSANs) existing in exclusive a mixture of C_s and C_{3h} keto-enamine tautomeric forms. In general, these star shaped mesogens are termed as hekates. Hekates mesogens (HMs) are novel materials that emit blue emission in contrast to other available DLCs exhibiting the green or red emissions [3, 4, 13].

ZnS quantum dots (QDs), a direct band-gap semiconductor of II−IV group, have drawn the attention of researchers in recent years due to their unique properties in chemical/biological sensing and photocatalysis arising from the size dependent quantum confinement effect [14, 15, 16, 17, 18]. The doping of any transition metal ions, like Mn^{2+}, in ZnS has also been emerged as a new method to tune the physical and luminescent properties of these QDs [15, 19, 20]. QDs are promising materials for doping in the liquid crystals [21] to achieve high photoluminescence (PL) intensity, good photo-stability and broad transforma-

2

tion of emission [22, 23, 24, 25, 26, 27, 28]. The doping of QDs in LCs has shown the tailoring of optical properties of host LCs [29, 30]. In 2012, Kumar et al. [27] have shown the enhancement in PL property of a ferroelectric liquid crystal (FLC) by doping with ZnS QDs. They stated that the emission of ZnS QDs combines constructively with that of the FLC to produce enhanced photoluminescence. Similar hypothesis has also been presented by Roy et al.[23] in which they demonstrated the tuning the photoluminescence of ZnS nanoflakes in the presence of an antiferroelectric liquid crystal into different concentrations. These reports could not be completely able to explain the reason of PL enhancement in the composites. In contrast, Singh et al. [31] have shown the quenching of normalized PL in a FLC by dispersing the host material with ZnS and $ZnS:Mn^{2+}$ QDs. During this quenching mechanism, the emission peaks remained at the same position and quenching has been found to be fairly depend upon the content of Mn. Dealing with a nematic LC and its reorientation in the presence of an external applied field, Kurochkina et al. [32] have successfully controlled the PL of host LC material by doping it with CdSe/ZnS; where they found the quenching of QDs luminescence with increasing electric field strength in the active LC matrix. The study of photoluminescence properties in LC and LC-composites is all-time interesting task in order to produce temperature stable highly luminescent displays [33]. All aforementioned studies are only limited to the nematic and ferroelectric phases of LC materials; therefore, the opportunity of such studies with other columnar LCs is still open [34]. Recently, we have performed the preparation of soft-nano composites of another star shaped mesogens with the insulating anatase TiO_2 nanoparticles and received interesting results in the form of triple photoluminescence which has shown significant quenching of PL with increasing temperature [35]. This study has left a plenty of opportunities to carry forward our investigation for the practical realization of high contrast photoluminescent displays using other nanomaterials.

With this in view, we have extended our studies on the photophysical properties of another family member of the star shaped hekates mesogens (HMs) derived from tris(N-salicylideneaniline) core with the dispersion of semiconductor

3

ZnS and ZnS:Mn^{2+} QDs. The characterization of QDs dispersed HMs composites has been carried out by using polarized optical microscopy, photoluminescence (PL) and Fourier-transform infrared (FTIR) spectroscopy. The change in mesogenic orientation due to the interactions between the guest QDs and the host HMs in hydogen bonded environment and variation of PL emission as a function of temperature have been analyzed and discussed within the scope of this paper.

2. Materials and methods

2.1. Star shaped mesogens

The liquid crystal used for the present investigation is DLT-10 (Figure 1). It is a star shaped liquid crystal material which is also known as hekates. DLT-10 refers to dialkoxy long armed tris(N-salicylideneaniline)s (TSANs), having ten number of carbon atoms in peripheral alkoxy chain [13]. This is a new class of mesogens occurring in the form of mixture comprising two inseparable keto enamine tautomers featuring C_{3h} and C_s rotational symmetries. This material is vital because of its blue emission in contrast to other conventional mesogens having red or green emissions. The phase transition sequence and corresponding enthalpies of DLT-10 material are given below-

$$Cr\ 77.4\ (0.9)\ Col_r\ 130.4\ (7.2)\ Col_h\ 169.6\ (3.8)\ I$$
$$I\ 166.7\ (3.6)\ Col_h\ 116.8\ (4.9)\ Col_r\ 56.1\ (11.4)\ Cr$$

All transition temperatures are presented in ^oC whereas corresponding transition enthalpies are mentioned in brackets with units in kJ/mol.

2.2. ZnS and ZnS:Mn^{2+} quantum dots

ZnS and 20 mol% Mn doped ZnS (ZnS:Mn^{2+}) quantum dots (QDs) were chosen as dopant to disperse in the aforementioned mesogens. The particle sizes (2r, diameter) of ZnS and ZnS:Mn^{2+} QDs were 2.25 and 2.45 nm, respectively [19, 31] which is smaller than the stacking distance, (i.e. 3.4 nm), of hekates-TSANs within the same column [13]. The absorption and emission wavelengths

4

of ZnS QDs were centered nearly at 300 and 400 nm, respectively. ZnS:Mn^{2+} QDs absorb the light of 312 nm and produce two PL emissions at 435 and 590 nm associated with the pristine ZnS and Mn incorporation in ZnS, respectively. Other details of these QDs have already been published in Refs.[19, 31]; therefore, the absorbance and PL curves of the pristine QDs are not given here.

2.3. Preparation of sample cells

ITO coated glass plates have been used to prepare the sample cells for polarized optical microscopic measurements. The active area of electrodes was taken to be 5×5 mm^2. The required pattern on ITO glass plates was obtained by the photolithography technique. Thickness of 5 μm between the both glass plates was uniformly maintained. The planar alignment on the patterned glass plates was obtained by using the conventional rubbed polyimide technique. The detailed information about the preparation of sample cells has been reported in our earlier published papers [31, 36, 37, 38, 39].

2.4. Preparation of DLT-10 hekates mesogens (HMs)-Quantum dots composites

ZnS and ZnS:Mn^{2+} quantum dots (QDs) suspensions were first prepared in toluene with a suspension concentration of 1 mg/ml followed by an ultrasonication for 1 hr to ensure the uniform and stable distribution of QDs in suspensions. Stability of all suspensions was checked by leaving those for one week under the ambient conditions. After confirming the stability of suspensions, we prepared the HMs-QDs composites. DLT-10 mesogens were also dissolved in toluene to maintain the experimental protocol in which ZnS and ZnS:Mn^{2+} QDs were added in a single concentration of 1.0 wt/wt %. These mixtures were subjected to ultrasonication for 30 min at isotropic temperature of DLT-10. The solvent was carefully evaporated from the composites and afterward, they were filled in sample cells by capillary method. The more details about the preparation of composites have already been reported by us [36, 38].

2.5. Polarized optical microscopy

QDs are well known dopant for altering the molecular orientation of liquid crystalline materials; therefore polarized optical microscopy was performed to analyze the change in the orientation of DLT-10 mesogens. The polarized optical micrographs (POMs) were recorded at 106 ^{o}C by using the polarized optical microscope, Radical RXLr-5. For this purpose, temperature of the sample cells was controlled by the INSTEC hot plate (HCS 302). The POMs were captured by an inbuilt digital camera (Jenoptix ProgresCT3) fixed at the top of microscope.

2.6. UV-visible, photoluminescence (PL) and Fourier-transform infrared (FTIR) study

UV-visible absorptions were recorded by using a UV-VIS Spectrophotometer (ELICO, SL 210). Photoluminescence spectra of the composites were performed at different temperatures between $30-90$ ^{o}C by using Agilent Cary Eclipse fluorescence spectrophotometer equipped with Xenon lamp of power 13 Watt (Cathodeon AXE 3u). 325 and 400 nm excitation wavelengths (λ_{ex}) and 10 nm slit width have been used for all PL measurements. Peltier based thermo-couple was used to maintain the temperature accuracy of $\pm$ 0.1 ^{o}C during PL measurements. Excitation wavelengths were selected according to the absorption characteristics of DLT-10 material. Fourier-transform Infrared (FTIR) spectroscopy was performed by using Shimadzu IR Affinity-I at room temperature.

3. Results and discussion

The dispersion of ZnS and ZnS:Mn^{2+} QDs significantly changes the molecular orientation of HMs which was confirmed by polarized optical microscopy. The polarized optical micrographs (POMs) are shown in Figure 2. POMs were recorded at 106 ^{o}C with a scale bar of 25 μm for all the samples. On adding ZnS QDs to DLT-10, a weak induced homeotropy in the molecular orientation can be observed (fig. 2b). In last decade, several research groups have reported
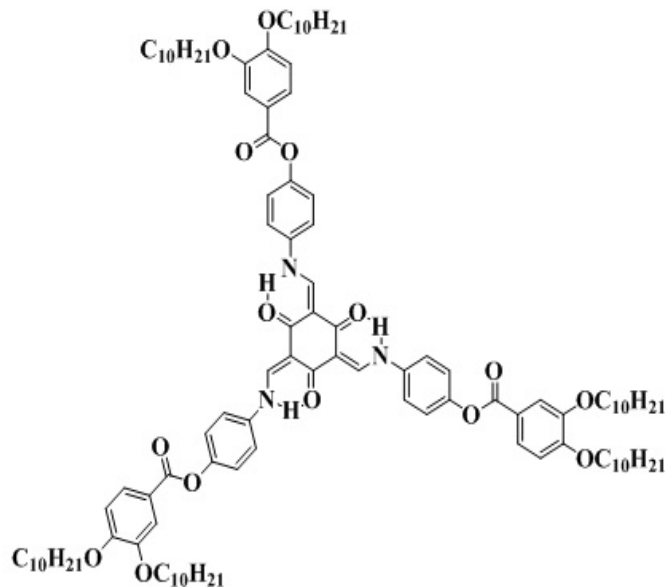
Figure 1: Molecular structure of star shaped hekates mesogen DLT-10.

the nanomaterials, like CdSe [40], CdSe/ZnS [41, 42], silica [43], gold [44, 45], based induced homeotropic orientation in different LC materials. In the present investigation, weak induced homeotropy in HMs has been observed by ZnS dispersion; in which ZnS QDs are expected to form a vertical self assembly which assists HMs to orient perpendicular to the substrate. In general, the optimized homeotropic alignment can be achieved if the length of mesogen is being on the order of tail. In addition to this, surface with strong polarity has also a tendency to induce homeotropic alignment. In our case, the size of QDs is smaller than that of the stacking distance of hekates-TSANs within the same column and no strong surface polarity takes place in composite. These two factors have caused a weak induced homeotropy in composite. The doping of Mn (20 mol %) in ZnS, enhances the dipolar interactions in ZnS:Mn^{2+} QDs [19, 31] and consequently results the formation of smaller columns of HMs,(visualized in fig. 2c), due to the effective short range interactions in HMs$-$ZnS:Mn^{2+} composite. The observed changes in POMs have again proven the self-assembling capability

of QDs in a soft mesogenic medium.

Absorption and PL emission spectra of the neat DLT-10 and DLT-10/QDs composites are shown in figure 3. The principal absorption band for DLT-10 is centered at 402 nm whereas, for DLT-10/QDs composites, it is hypsochromic (blue) shifted by 46 nm and observed at 356 nm. DLT-10 shows two absorption peaks at 324 and 402 nm attributed to $\pi-\pi^*$ and $n-\pi^*$ transitions, respectively [13]. The absorption wavelengths for ZnS and ZnS:Mn^{2+} QDs are reported at 305 and 312 nm, respectively (See supplementary Figure S1)[19]. In QDs, absorption band is analogous to the bandgap of QDs and the blue/red shift in the absorption spectra is a consequence of quantum confinement effect [46]. In our investigation, the observed hypsochromic shift in the absorption spectra of DLT-10/QDs composites is due to the formation of hybrid system and partial overlapping of the absorptions bands of pristine QDs and $\pi-\pi^*$ absorption band of the DLT-10 HMs. It should be noticed that the host DLT-10 matrix represents a supramolecular system and not referred to be a quantum mechanical confined matrix; therefore the shift in photophysical (absorption/emission) properties is not related to any quantum confinement effects. It is also observed that the magnitude of absorption of the DLT-10/QDs composites has been diminished in comparison to the pure DLT-10 HMs which is probably due to the mismatching of the absorption bands of the DLT-10 and QDs. In the DLT-10/QDs composites, QDs behave like impurity additives that reduces the absorption property.

PL study of neat DLT-10 and its composites with ZnS and ZnS:Mn^{2+} QDs has been carried out in the solution state which is shown in figure 3. It is reported by Goel et al. [47] that the PL emission of ferroelectric $LC-CeO_2$ system remarkably depends on the excitation wavelength; therefore, we have also examined this effect. Two excitation wavelengths (i.e. 325 and 400 nm) have been selected for this purpose and we found that the change in excitation wavelength only changes the intensity of emission (see supplementary fig. S2). When we excite a fluorescent material, some energy is dissipated leaving the fluorophore in the lowest vibrational level. This relaxation takes place in 10^{-12}
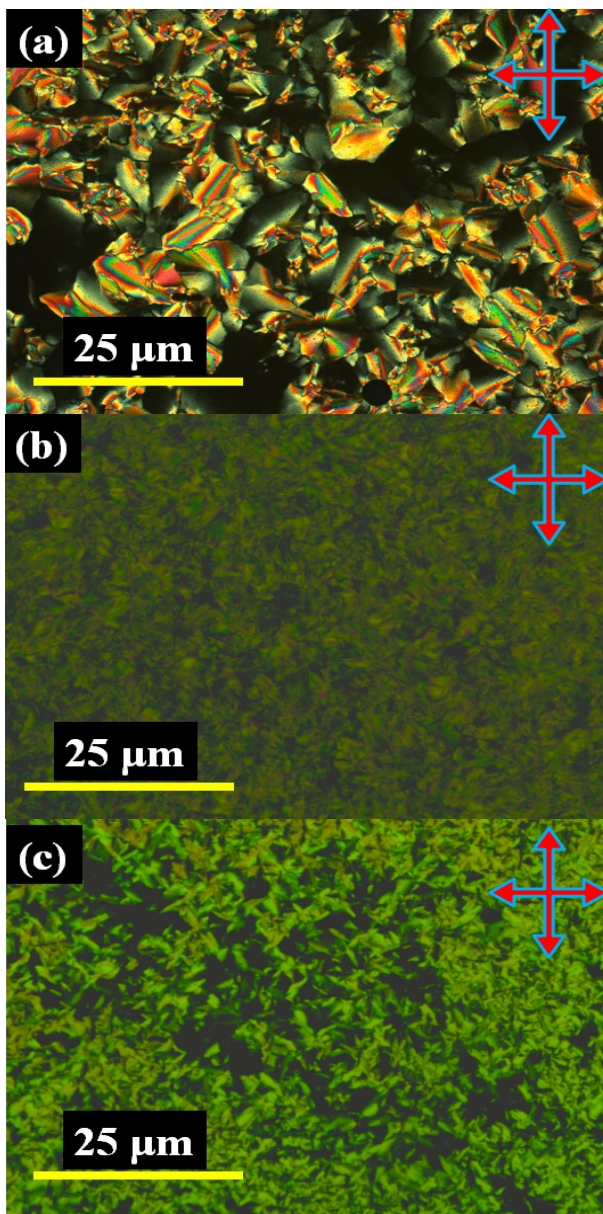
Figure 2: Polarized optical micrographs of (a) DLT-10, (b) DLT-10 dispersed with ZnS QDs and (c) DLT-10 dispersed with ZnS:Mn^{2+} QDs at 106 ^{o}C.
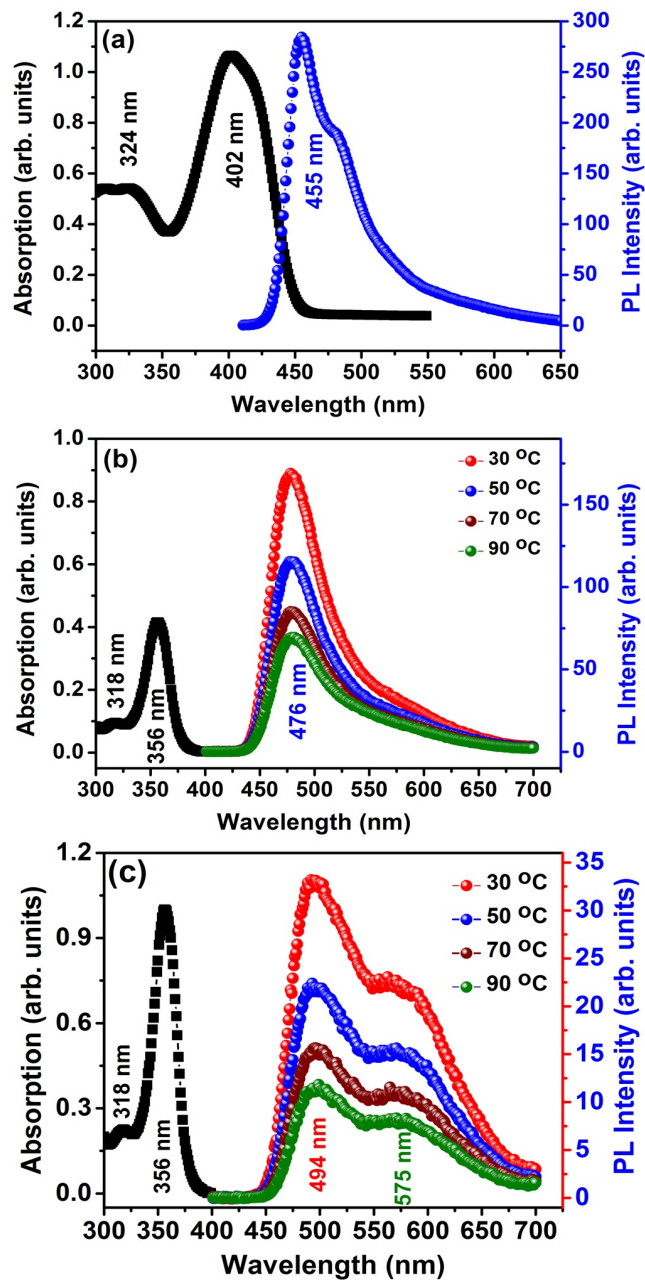
Figure 3: Absorption and emission of (a) DLT-10, (b) DLC-10 dispersed with ZnS QDs and (c) DLC-10 dispersed with ZnS:Mn^{2+} QDs.

seconds which is presumably a result of a strong overlap among numerous states of nearly equal energy. Due to this rapid relaxation, emission spectra are invariant of the excitation wavelength. For recording the PL spectra of neat DLT-10 and its composites with QDs, 400 nm wavelength was taken as excitation source. This selection criterion was chosen to observe the PL emission that corresponds to n$-\pi$* absorption transition of neat DLT-10 HMs, so that we could only excite to the DLT-10 HMs. By only exciting DLT-10 HMs, we can investigate the influence of QDs on the PL properties of HMs without activating the fluorescence of pristine QDs. It is clear from figure 3 that the neat DLT-10 HMs transmit blue emission of wavelength 455 nm with a negligible shoulder when their solutions were irradiated with 400 nm absorption maximum. The blue emission of DLT-10 is attributed to the electron$-$proton interaction in the hydrogen bonding environment and quenches with the increase in temperature. The detailed PL emission and its thermal quenching mechanism have already been reported in ref.[13]; therefore, we only presented a single emission of DLT-10 recorded at 30 ^{o}C.

After the dispersion of ZnS QDs in DLT-10 HMs, the PL emission has been observed to be red-shifted and centered at 476 nm. In addition, PL emission has also been enhanced which quenches with increasing temperature. DLT-10 HMs are capable to make hydrogen-bonded environment in solution state in which electron-proton interactions become stronger due to the dispersion of ZnS QDs that gives enhanced PL in the composite. As ZnS QDs also exhibit PL emission at 400 nm; therefore, the second possible reason for the enhancement in PL can be the exciton resonance between the individual PL emissions of ZnS QDs and DLT-10.

The doping of Mn^{2+} ions in ZnS QDs introduces a secondary yellow emission at 590 nm including a principal blue emission at 435 nm. This secondary emission is either attributed to the formation of Mn^{2+} luminescent centers in the ZnS:Mn^{2+} QDs or $^{4}T_1$ to $^{6}A_1$ transition between the sp electrons of ZnS and d electrons of Mn^{2+}; but the origin of this emission is still controversial. It is well known fact that Mn has d^5 electronic structure with tetrahedral symme-

try [19, 31]. When Mn^{2+} ions are incorporated in ZnS, they occupy the certain sites of Zn^{2+} and mixing between s-p electron of ZnS and d electron of Mn^{2+} takes place. Therefore, forbidden transitions are partially allowed giving rise to Mn^{2+} related yellow color PL emission. Borse et al. [20] have also reported that the large content of Mn in ZnS causes $^4T_1$ to $^6A_1$ transitions between the sp electrons of ZnS and d electrons of Mn^{2+}, which results an additional emission band near 600 nm. In DLT-10 HMs$-$ZnS:Mn^{2+} QDs composite, two emission peaks have been noticed at 494 and 575 nm, respectively. The first emission peak at 494 nm is analogous to principal blue emission wheras secondary emission at 575 nm is attributed to $^4T_1$ to $^6A_1$ transitions in ZnS:Mn^{2+} QDs. The temperature dependence of PL emission for DLT-10 HMs/QDs composites is also clear in figure 3. Thermal quenching fairly follows the Seitz relation [48]-

$$I(T) = \frac{I_o}{1 + A\exp(-E_b/kT)} \tag{1}$$

where, E_b is the activation energy known as the thermal quenching energy, k is the Boltzmann constant, A is a constant related to the ratio of the non$-$radiative to the radiative recombination rate, and I_o is the emission intensity at 0 K.

The quantum yield (QY) of the neat DLT-10 and DLT-10/QDs composites has been measured at 30 ^{o}C by calculating the integrated intensity of the absorbance and emission spectra [49]. The QY has been calculated with respect to toluene. The relative QY for the neat DLT-10 HMs [6] and DLT-10 HMs/QDs composite with the dispersion of ZnS QDs and QYs were found to be 0.29 and 0.73, respectively. The QY for the DLT-10/ZnS:Mn^{2+} could not be determined due to the interference of the secondary emission at 575 nm. Accurate calculation of the relative quantum yields is difficult because of the need to correct for the changing absorbance of the solution[49].

Figure 4 depicts the Stokes shift (in nm) in DLT-10 and its composites with QDs. The Stokes shift is the difference between the spectral positions of the band maxima of absorption and emission spectra for the same electronic transitions
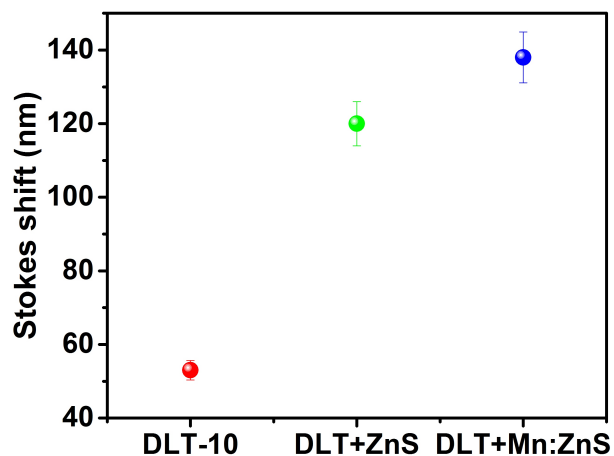
Figure 4: Stokes shift of pure DLT-10 and it's composite with QDs.

that signifies the Energy losses during the excitation and emission processes. The Stokes shifts for DLT-10 and its composites with ZnS and ZnS:Mn^{2+} QDs have been found to be 53, 120 and 138 nm, respectively. In DLT-10/QDs composites, the enhanced Stokes shift and the redshift in the emission band are in agreement with the general experimental observation; suggesting that the strong intermolecular interactions take place in the composites. Koda et al. [50] have reported that the shift in the emission peak can also be observed if the guest dopant occupies few certain positions in the host structure. Taking this theory into account, we can also explain the red-shift in PL emission. ZnS and ZnS:Mn^{2+} QDs can occupy certain sites at the DLT-10 HMs which redistribute liquid crystalline (mesogenic) field strength. In pure DLT-10, the mesogenic field strength depends on the degree of interactions between two mesogenic molecules. After the dispersion of QDs in DLT-10 host matrix, this field strength is influenced by the Guest-Host interactions in composites. In QDs/DLT-10 composites, the mesogenic-mesogenic interactions (interaction between two successive DLT-10 molecules) are reduced in comparison to the Guest-Host interactions between QDs and DTL-10 molecules which cause a red shift in the PL.

The physical interactions between DLT-10 HMs and QDs have been analyzed
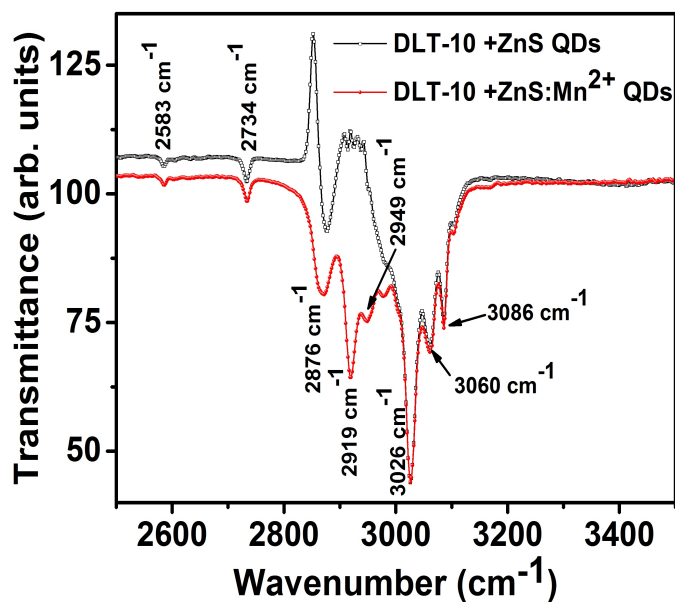
Figure 5: Fourier-transformed infrared (FTIR) spectra of DLT-10 dispersed with QDs.

by using the FTIR spectroscopy. The FTIR spectra of DLT-10/QDs composites are shown in figure 5. The FTIR spectra were recorded for the wave number interval of $1500-4000$ cm^{-1} in solution state by taking toluene as solvent. It is observed that the vibrational bands of DLT-10 HMs between $2500-3500$ cm^{-1} have been modified with the dispersion of QDs. Yelamaggad et al.[13] have shown that the DLT-10 HMs exhibit three major vibration bands nearly at $\approx$ 3334, 2924 and 2854 cm^{-1} corresponding to N$-$H stretching, CH$_2$/CH$_3$ asymmetric and symmetric stretching vibrations, respectively (see supplementary fig. S3).

In DLT-10 HMs/QDs composites, the N$-$H stretching, CH$_2$/CH$_3$ asymmetric and symmetric stretching vibrations have been shifted in comparison to pure DLT-10 HMs and found to be at 3026, 2919 and 2876 cm^{-1}, respectively. The large shift in N$-$H stretching band reveals the formation of composite [51]. In addition, a new induced band at 2734 cm^{-1} in DLT-10 HMs/QDs composites is analogous to the induced S$-$H stretching, between the QDs and DLT-10 HMs.

14

In addition, Liu et al.[52] have also shown that an induced S−H stretching band can be observed nearly at 2500 cm^{-1} in the thiol-functionalized mesoporous calcium silicate which supports our hypothesis about the induced S−H stretching band in the DLT-10 HMs/QDs composite.

4. Conclusions

In summary, the photophysical properties of the star shaped hekates mesogens (HMs) derived from tris(N-salicylideneaniline)s core have been investigated in the presence of an optimized concentration of ZnS and ZnS:Mn^{2+} QDs. The neat DLT-10 HMs and its composites with QDs have been characterized by polarized optical microscopy, UV-visible, photoluminescence and Fourier-transform infrared (FTIR) spectroscopy. Polarized optical microscopy has revealed that ZnS QDs significantly changes the orientation of HMs by inducing a weak homeotropy whereas ZnS:Mn^{2+} QDs break HMs in smaller columns due to the effective short range interactions. The neat DLT-10 HMs show two absorption peaks located at 324 and 402 nm attributed to $\pi-\pi$* and n$-\pi$* transitions, respectively and transmit blue emission at 455 nm. The dispersion of ZnS QDs leads to the enhancement in the PL properties of DLT-10 which is analogous to the strengthening of electron-proton interactions in the hydrogen bonded environment of HMs. In addition, the presence of ZnS QDs causes a red-shift in the blue emission of HMs. The relative quantum yields (QY) of the neat DLT-10 HMs and DLT-10 HMs/QDs composite with the dispersion of ZnS QDs and QYs were found to be 0.29 and 0.73, respectively. The presence of ZnS:Mn^{2+} QDs in DLT-10 offers two emissions; blue emission at 494 nm and yellow emission at 575 nm. The yellow emission at 575 nm is attributed to the ^{4}T$_1$ to ^{6}A$_1$ transition between the sp electrons of ZnS and d electrons of Mn^{2+}. The Stokes shift in DLT-10 HMs/QDs composite is found to be increased because of the re-distribution of liquid crystalline field strength by affecting the effective ionic contributions in composites. The significant shift in N−H stretching band and induction of a new S−H stretching band at 2734 cm^{-1} have confirmed the ex-

istence of intermolecular interactions between the DLT-10 HMs and QDs. The present study reveals that HMs/QDs composites are superior to be used in the luminescent displays. The tunability of blue emission of neat HMs will certainly open a new scope for the optical devices.

Acknowledgements

References

[1] S. Sergeyev, W. Pisula, Y. H. Geerts, Discotic liquid crystals: a new generation of organic semiconductors, Chemical Society Reviews 36 (12) (2007) 1902–1929. `doi:10.1039/B417320C`.
URL `http://pubs.rsc.org/en/content/articlelanding/2007/cs/b417320c`

[2] S. Kumar, Chemistry of Discotic Liquid Crystals: From Monomers to Polymers (Dec. 2010).
URL `https://www.crcpress.com/Chemistry-of-Discotic-Liquid-Crystals-From-Monomers-to-Pol Kumar/p/book/9781439811436`

[3] M. Pope, C. E. Swenberg, Electronic Processes in Organic Crystals and Polymers, second edition Edition, Monographs on the Physics and Chemistry of Materials, Oxford University Press, Oxford, New York, 1999.

[4] Q. Li, Self-Organized Organic Semiconductors: From Materials to Device Applications (Apr. 2011).
URL `https://www.wiley.com/en-us/Self+Organized+`

Organic+Semiconductors%3A+From+Materials+to+Device+
Applications-p-9780470559734

[5] P. L. Madhuri, D. S. S. Rao, C. V. Yelamaggad, A. S. Achalkumar, S. K. Prasad, Fast Photoluminescence Switching in the Nematic Phase of CalamiticDiscotic Composites, Advanced Optical Materials 3 (8) (2015) 1116–1124. `doi:10.1002/adom.201500126`.
URL `https://onlinelibrary.wiley.com/doi/abs/10.1002/adom.201500126`

[6] A. S. Achalkumar, B. N. Veerabhadraswamy, U. S. Hiremath, D. S. S. Rao, S. K. Prasad, C. V. Yelamaggad, Photoluminescent discotic liquid crystals derived from tris(N-salicylideneaniline) and stilbene conjugates: Structureproperty correlations, Dyes and Pigments 132 (2016) 291–305. `doi:10.1016/j.dyepig.2016.05.010`.
URL `http://www.sciencedirect.com/science/article/pii/S0143720816302005`

[7] B. R. Kaafarani, Discotic Liquid Crystals for Opto-Electronic Applications, Chemistry of Materials 23 (3) (2011) 378–396. `doi:10.1021/cm102117c`.
URL `https://doi.org/10.1021/cm102117c`

[8] D. Adam, P. Schuhmacher, J. Simmerer, L. Hussling, K. Siemensmeyer, K. H. Etzbachi, H. Ringsdorf, D. Haarer, Fast photoconduction in the highly ordered columnar phase of a discotic liquid crystal, Nature 371 (6493) (1994) 141–143. `doi:10.1038/371141a0`.
URL `https://www.nature.com/articles/371141a0`

[9] X. Feng, V. Marcon, W. Pisula, M. R. Hansen, J. Kirkpatrick, F. Grozema, D. Andrienko, K. Kremer, K. Mllen, Towards high charge-carrier mobilities by rational design of the shape and periphery of discotics, Nature Materials 8 (5) (2009) 421–426. `doi:10.1038/nmat2427`.
URL `https://www.nature.com/articles/nmat2427`

[10] K. P. Gan, M. Yoshio, Y. Sugihara, T. Kato, Guanineoligothiophene conjugates: liquid-crystalline properties, photoconductivities and ion-responsive emission of their nanoscale assemblies, Chemical Science 9 (3) (2018) 576–585. doi:10.1039/C7SC03764C.
URL http://pubs.rsc.org/en/content/articlelanding/2018/sc/c7sc03764c

[11] W. Zhang, S. Zhang, Z. Zhang, H. Yang, A. Zhang, X. Hao, J. Wang, C. Zhang, J. Pu, 2d Organic Superlattice Promoted via Combined Action of Stacking and DipoleDipole Interaction in Discotic Liquid Crystals, The Journal of Physical Chemistry B 121 (31) (2017) 7519–7525. doi:10.1021/acs.jpcb.7b05465.
URL https://doi.org/10.1021/acs.jpcb.7b05465

[12] A. Gowda, L. Jacob, D. P. Singh, R. Douali, S. Kumar, Charge Transport in Novel Phenazine Fused Triphenylene Supramolecular Systems, ChemistrySelect 3 (23) (2018) 6551–6560. doi:10.1002/slct.201801412.
URL https://onlinelibrary.wiley.com/doi/abs/10.1002/slct.201801412

[13] A. S. Achalkumar, U. S. Hiremath, D. S. S. Rao, S. K. Prasad, C. V. Yelamaggad, Self-Assembly of Hekates-Tris(N-salicylideneaniline)s into Columnar Structures: Synthesis and Characterization, The Journal of Organic Chemistry 78 (2) (2013) 527–544. doi:10.1021/jo302332u.
URL https://doi.org/10.1021/jo302332u

[14] J. F. Suyver, R. Meester, J. J. Kelly, A. Meijerink, A theory waiting for an experiment: pair-state formation in a nanocrystal, Journal of Luminescence 102-103 (2003) 182–188. doi:10.1016/S0022-2313(02)00487-8.
URL http://www.sciencedirect.com/science/article/pii/S0022231302004878

[15] A. K. Kole, P. Kumbhakar, Effect of manganese doping on the photoluminescence characteristics of chemically synthesized zinc

sulfide nanoparticles, Applied Nanoscience 2 (1) (2012) 15–23. doi:10.1007/s13204-011-0036-x.
URL https://link.springer.com/article/10.1007/s13204-011-0036-x

[16] T. T. Q. Hoa, N. D. The, S. McVitie, N. H. Nam, L. V. Vu, T. D. Canh, N. N. Long, Optical properties of Mn-doped ZnS semiconductor nanoclusters synthesized by a hydrothermal process, Optical Materials 33 (3) (2011) 308–314. doi:10.1016/j.optmat.2010.09.008.
URL http://www.sciencedirect.com/science/article/pii/S0925346710003927

[17] X. Fang, Y. Bando, M. Liao, T. Zhai, U. K. Gautam, L. Li, Y. Koide, D. Golberg, An Efficient Way to Assemble ZnS Nanobelts as Ultraviolet-Light Sensors with Enhanced Photocurrent and Stability, Advanced Functional Materials 20 (3) (2010) 500–508. doi:10.1002/adfm.200901878.
URL https://onlinelibrary.wiley.com/doi/abs/10.1002/adfm.200901878

[18] J. H. He, Y. Y. Zhang, J. Liu, D. Moore, G. Bao, Z. L. Wang, ZnS/Silica Nanocable Field Effect Transistors as Biological and Chemical Nanosensors, The Journal of Physical Chemistry C 111 (33) (2007) 12152–12156. doi:10.1021/jp074772u.
URL https://doi.org/10.1021/jp074772u

[19] A. K. Kole, C. S. Tiwary, P. Kumbhakar, Room temperature synthesis of Mn2+ doped ZnS d-dots and observation of tunable dual emission: Effects of doping concentration, temperature, and ultraviolet light illumination, Journal of Applied Physics 113 (11) (2013) 114308. doi:10.1063/1.4795779.
URL https://aip.scitation.org/doi/abs/10.1063/1.4795779

[20] P. H. Borse, D. Srinivas, R. F. Shinde, S. K. Date, W. Vogel, S. K. Kulkarni, Effect of ${\mathrm{Mn}}^{2+}$ concentration in ZnS nanoparticles on

photoluminescence and electron-spin- resonance spectra, Physical Review B 60 (12) (1999) 8659–8664. `doi:10.1103/PhysRevB.60.8659`.
URL `https://link.aps.org/doi/10.1103/PhysRevB.60.8659`

[21] J. Mirzaei, M. Reznikov, T. Hegmann, Quantum dots as liquid crystal dopants, Journal of Materials Chemistry 22 (42) (2012) 22350–22365. `doi:10.1039/C2JM33274D`.
URL `http://pubs.rsc.org/en/content/articlelanding/2012/jm/c2jm33274d`

[22] J. S. Roy, T. P. Majumder, R. Dabrowski, Enhanced photoluminescence in CdS nanorods doped with antiferroelectric liquid crystals, Journal of Luminescence 148 (2014) 330–333. `doi:10.1016/j.jlumin.2013.12.045`.
URL `http://www.sciencedirect.com/science/article/pii/S0022231313008818`

[23] J. S. Roy, T. Pal Majumder, R. Dbrowski, A. Dey, P. P. Ray, Tuning photoluminescence of liquid crystals doped ZnS nanoflakes, Optical Materials 46 (2015) 467–471. `doi:10.1016/j.optmat.2015.05.005`.
URL `http://www.sciencedirect.com/science/article/pii/S0925346715002955`

[24] T. Joshi, P. Ganguly, D. Haranath, S. Singh, A. M. Biradar, Tuning the photoluminescence of ferroelectric liquid crystal by controlling the size of dopant ZnO quantum dots, Materials Letters 114 (2014) 156–158. `doi:10.1016/j.matlet.2013.09.110`.
URL `http://www.sciencedirect.com/science/article/pii/S0167577X13013542`

[25] J. S. Roy, T. Pal Majumder, R. Dabrowski, Photoluminescence behavior of TiO2 nanoparticles doped with liquidcrystals, Journal of Molecular Structure 1098 (2015) 351–354. `doi:10.1016/j.molstruc.2015.06.028`.
URL `http://www.sciencedirect.com/science/article/pii/S0022286015300533`

[26] S. Doke, K. Sonawane, V. R. Reddy, P. Ganguly, S. Mahamuni, Low power operated highly luminescent ferroelectric liquid crystal doped with CdSe/ZnSe core/shell quantum dots, Liquid Crystals 0 (0) (2018) 1–7. doi:10.1080/02678292.2018.1449260.
URL https://doi.org/10.1080/02678292.2018.1449260

[27] A. Kumar, J. Prakash, A. D. Deshmukh, D. Haranath, P. Silotia, A. M. Biradar, Enhancing the photoluminescence of ferroelectric liquid crystal by doping with ZnS quantum dots, Applied Physics Letters 100 (13) (2012) 134101. doi:10.1063/1.3698120.
URL https://aip.scitation.org/doi/full/10.1063/1.3698120

[28] T. Vimal, D. P. Singh, K. Agrahari, A. Srivastava, R. Manohar, Analysis of optical properties and mechanism of photoluminescence enhancement of quantum dot - ferroelectric liquid crystal composite, Photonics Letters of Poland 8 (1) (2016) 23–25. doi:10.4302/photon.lett.pl.v8i1.609.
URL http://photonics.pl/PLP/index.php/letters/article/view/8-9

[29] A. Kumar, S. Tripathi, A. D. Deshmukh, D. Haranath, P. Singh, A. M. Biradar, Time evolution photoluminescence studies of quantum dot doped ferroelectric liquid crystals, Journal of Physics D: Applied Physics 46 (19) (2013) 195302. doi:10.1088/0022-3727/46/19/195302.
URL http://stacks.iop.org/0022-3727/46/i=19/a=195302

[30] N. A. Shurpo, M. S. Vakshtein, N. V. Kamanina, Effect of CdSe/ZnS semiconductor quantum dots on the dynamic properties of nematic liquid-crystalline medium, Technical Physics Letters 36 (4) (2010) 319–321. doi:10.1134/S1063785010040097.
URL https://link.springer.com/article/10.1134/S1063785010040097

[31] D. P. Singh, A. Daoudi, S. K. Gupta, S. Pandey, T. Vimal, R. Manohar, A. K. Kole, P. Kumbhakar, A. Kumar, Mn2+ doped ZnS quantum dots

21

in ferroelectric liquid crystal matrix: Analysis of new relaxation phenomenon, faster optical response, and concentration dependent quenching in photoluminescence, Journal of Applied Physics 119 (9) (2016) 094101. `doi:10.1063/1.4942663`.

URL `https://aip.scitation.org/doi/abs/10.1063/1.4942663`

[32] M. A. Kurochkina, E. A. Konshina, D. Khmelevskaia, Photoluminescence of CdSe/ZnS quantum dots in nematic liquid crystals in electric fields, Beilstein Journal of Nanotechnology 9 (1) (2018) 1544–1549. `doi:10.3762/bjnano.9.145`.

URL `https://www.beilstein-journals.org/bjnano/articles/9/145`

[33] D. P. Singh, B. Duponchel, Y. Boussoualem, K. Agrahari, R. Manohar, V. Kumar, R. Pasricha, G. H. Pujar, S. R. Inamdar, R. Douali, A. Daoudi, Dual photoluminescence and charge transport in an alkoxy biphenyl benzoate ferroelectric liquid crystallinegraphene oxide composite, New Journal of Chemistry 42 (20) (2018) 16682–16693. `doi:10.1039/C8NJ02985G`.

URL `https://pubs.rsc.org/en/content/articlelanding/2018/nj/c8nj02985g`

[34] Y. H. Kim, D. K. Yoon, E. H. Lee, Y. K. Ko, H.-T. Jung, Photoluminescence Properties of a Perfluorinated Supramolecular Columnar Liquid Crystal with a Pyrene Core: Effects of the Ordering and Orientation of the Columns, The Journal of Physical Chemistry B 110 (42) (2006) 20836–20842. `doi:10.1021/jp063115j`.

URL `https://doi.org/10.1021/jp063115j`

[35] D. P. Singh, K. Agrahari, A. S. Achalkumar, C. V. Yelamaggad, R. Manohar, M. Depriester, Preparation and photophysical properties of soft-nano composites comprising guest anatase TiO_2 nanoparticle and host hekates mesogens, Journal of Luminescence 205 (2019) 304–309. `doi:10.1016/j.jlumin.2018.09.035`.

URL   http://www.sciencedirect.com/science/article/pii/
S0022231318310755

[36] D. P. Singh, S. Pandey, S. K. Gupta, R. Manohar, A. Daoudi, A. H.
Sahraoui, C. Phadnis, S. Mahamuni, Quenching of photoluminescence
and enhanced contrast of ferroelectric liquid crystal dispersed with
Cd1XZnXS/ZnS core/shell nanocrystals, Journal of Luminescence 173
(2016) 250–256. doi:10.1016/j.jlumin.2015.12.042.
URL   http://www.sciencedirect.com/science/article/pii/
S0022231315301393

[37] A. K. Misra, P. K. Tripathi, R. Manohar, Reduction of optical response
time for fluorescent dye doped ferroelectric liquid crystal, Journal of Molec-
ular Liquids 175 (2012) 67–71. doi:10.1016/j.molliq.2012.08.016.
URL   http://www.sciencedirect.com/science/article/pii/
S0167732212003054

[38] D. P. Singh, S. Pandey, R. Manohar, S. Kumar, G. H. Pujar, S. R. Inam-
dar, Time-resolved fluorescence and absence of Frster resonance energy
transfer in ferroelectric liquid crystal-quantum dots composites, Journal of
Luminescence 190 (2017) 161–170. doi:10.1016/j.jlumin.2016.09.056.
URL   http://www.sciencedirect.com/science/article/pii/
S0022231316300369

[39] A. K. Misra, P. K. Tripathi, R. Manohar, Fluorescence, UV ab-
sorbance and dielectric studies of fluorescent dye doped ferroelec-
tric liquid crystal, Journal of Non-Crystalline Solids 412 (2015) 1–4.
doi:10.1016/j.jnoncrysol.2014.11.037.
URL   http://www.sciencedirect.com/science/article/pii/
S0022309314006401

[40] D. P. Singh, S. K. Gupta, R. Manohar, M. C. Varia, S. Kumar, A. Kumar,
Effect of cadmium selenide quantum dots on the dielectric and physical
parameters of ferroelectric liquid crystal, Journal of Applied Physics 116 (3)

(2014) 034106. `doi:10.1063/1.4890352`.
URL `https://aip.scitation.org/doi/abs/10.1063/1.4890352`

[41] E. Petrescu, C. Cirtoaje, O. Danila, Dynamic behavior of nematic liquid crystal mixtures with quantum dots in electric fields, Beilstein Journal of Nanotechnology 9 (1) (2018) 399–406. `doi:10.3762/bjnano.9.39`.
URL `https://www.beilstein-journals.org/bjnano/articles/9/39`

[42] A. L. Rodarte, F. Cisneros, J. E. Hein, S. Ghosh, L. S. Hirst, Quantum Dot/Liquid Crystal Nanocomposites in Photonic Devices, Photonics 2 (3) (2015) 855–864. `doi:10.3390/photonics2030855`.
URL `http://www.mdpi.com/2304-6732/2/3/855`

[43] P. Kumar, S. Y. Oh, V. K. Baliyan, S. Kundu, S. H. Lee, S.-W. Kang, Topographically induced homeotropic alignment of liquid crystals on self-assembled opal crystals, Optics Express 26 (7) (2018) 8385–8396. `doi:10.1364/OE.26.008385`.
URL `https://www.osapublishing.org/oe/abstract.cfm?uri=oe-26-7-8385`

[44] H. Qi, T. Hegmann, Liquid crystalgold nanoparticle composites, Liquid Crystals Today 20 (4) (2011) 102–114. `doi:10.1080/1358314X.2011.610133`.
URL `https://doi.org/10.1080/1358314X.2011.610133`

[45] M. Urbanski, J. Mirzaei, T. Hegmann, H.-S. Kitzerow, Nanoparticle Doping in Nematic Liquid Crystals: Distinction between Surface and Bulk Effects by Numerical Simulations, ChemPhysChem 15 (7) (2014) 1395–1404. `doi:10.1002/cphc.201301054`.
URL `https://onlinelibrary.wiley.com/doi/abs/10.1002/cphc.201301054`

[46] D. V. Talapin, J.-S. Lee, M. V. Kovalenko, E. V. Shevchenko, Prospects of Colloidal Nanocrystals for Electronic and Optoelectronic Applications,

Chemical Reviews 110 (1) (2010) 389–458. `doi:10.1021/cr900137k`.
URL `https://doi.org/10.1021/cr900137k`

[47] P. Goel, M. Arora, A. M. Biradar, Evolution of excitation wavelength dependent photoluminescence in nano-CeO2 dispersed ferroelectric liquid crystals, RSC Advances 4 (22) (2014) 11351–11356. `doi:10.1039/C3RA47225F`.
URL `http://pubs.rsc.org/en/content/articlelanding/2014/ra/c3ra47225f`

[48] F. Seitz, An interpretation of crystal luminescence, Transactions of the Faraday Society 35 (0) (1939) 74–85. `doi:10.1039/TF9393500074`.
URL `http://pubs.rsc.org/en/content/articlelanding/1939/tf/tf9393500074`

[49] J. R. Lakowicz, Principles of Fluorescence Spectroscopy, 3rd Edition, Springer US, 2006.
URL `//www.springer.com/fr/book/9780387312781`

[50] Takao Koda, Shigeo Shionoya, Masamichi Ichikawa, Shigeru Minomura, Effect of pressure on the luminescence of zinc sulphide phosphors, Journal of Physics and Chemistry of Solids 27 (10) (1966) 1577–1586. `doi:10.1016/0022-3697(66)90235-6`.
URL `http://www.sciencedirect.com/science/article/pii/0022369766902356`

[51] M. Garcia-Cortes, E. Sotelo Gonzlez, M. T. Fernndez-Argelles, J. R. Encinar, J. M. Costa-Fernndez, A. Sanz-Medel, Capping of Mn-Doped ZnS Quantum Dots with DHLA for Their Stabilization in Aqueous Media: Determination of the Nanoparticle Number Concentration and Surface Ligand Density, Langmuir 33 (25) (2017) 6333–6341. `doi:10.1021/acs.langmuir.7b00409`.
URL `https://doi.org/10.1021/acs.langmuir.7b00409`

[52] L. Lihua, T. Li, G. Yang, Y. Wang, A. Tang, Y. Ling, Synthesis of thiol-functionalized mesoporous calcium silicate and its adsorption characteristics for heavy metal ions, Journal of Environmental Chemical Engineering 5 (6) (2017) 6201–6215. `doi:10.1016/j.jece.2017.11.046`.
URL `http://www.sciencedirect.com/science/article/pii/S2213343717306048`

Graphical Abstract